AIAA 2002-2203
Thermophysics Characterization of Multiply Ionized Air Plasma Absorption of Laser Radiation

Ten-See Wang
NASA Marshall Space Flight Center
Huntsville, AL

Robert Rhodes
The University of Tennessee Space Institute
Tullahoma, TN

33rd AIAA Plasmadynamics and Lasers Conference
20-23 May 2002 / Maui, Hawaii

AIAA 2002-2203

Thermophysics Characterization of Multiply Ionized Air Plasma Absorption of Laser Radiation

Ten-See Wang*
NASA Marshall Space Flight Center, Huntsville, AL 35812
and
Robert Rhodes†
The University of Tennessee Space Institute, TN 37388

Abstract

The impact of multiple ionization of air plasma on the inverse Bremsstrahlung absorption of laser radiation is investigated for air breathing laser propulsion. Thermo-chemical properties of multiply ionized air plasma species are computed for temperatures up to 200,000 deg K, using hydrogenic approximation of the electronic partition function; And those for neutral air molecules are also updated for temperatures up to 50,000 deg K, using available literature data. Three formulas for absorption are calculated and a general formula is recommended for multiple ionization absorption calculation. The plasma composition required for absorption calculation is obtained by increasing the degree of ionization sequentially, up to quadruple ionization, with a series of thermal equilibrium computations. The calculated second ionization absorption coefficient agrees reasonably well with that of available data. The importance of multiple ionization modeling is demonstrated with the finding that area under the quadruple ionization curve of absorption is found to be twice that of single ionization. The effort of this work is beneficial to the computational plasma aerodynamics modeling of laser lightcraft performance.

Nomenclature

a_0	first Bohr radius
$a_1 - a_7$	coefficients for thermodynamic functions
b_1, b_2	thermodynamic function integration constants
c	light velocity in vacuum
C_p	molar heat capacity at constant pressure
e	proton charge
E	ionization potential
E_l	lowering of the ionization potential
G	Gaunt factor
h	Plank Constant
I	laser intensity
H	molar enthalpy at temperature for standard state
H_0	molar enthalpy at 0 K for standard state
m_e	electron mass
n	nth state of excitation energy
n_e, n_i	number density of electron and ions
n_a, n_m	number density of atoms and molecules
Q	partition function
p	pressure
R	universal gas constant
S	entropy at temperature for standard state
s_c	Sackur-Tetrode constant
s_i	optical path length of the ith ray
T	temperature
Z	ion charge

Greek Symbols

α	fine structure constant
κ	absorption coefficient
κ_B	Boltzmann's constant
ε_0	permittivity of free space
$\hbar$	Plank constant / 2π
μ	real refractive index
ω	angular frequency

Subscripts

e	electron
i	ith state

Introduction

Kantrowitz[1] first suggested a new possibility for dramatic cost reductions in mass launching to Earth orbit

* Staff, Applied Fluid Dynamics Analysis Group, Senior Member AIAA
† Senior Scientist, Member AIAA

with a ground-based high-power laser in the 70's. Since then, a propulsion system supported by a laser-sustained plasma has been the subject of many researches.[P1,G1,B1,P2] The main advantage gained by laser propulsion over chemical propulsion is the low-weight system obtained from decoupling the energy source from the vehicle, and high specific impulse resulting in low fuel consumption. In addition, the flame temperature of a combustion process is limited, whereas the propellant temperature reachable during laser propulsion can be several order-of-magnitude higher.

Several air-breathing laser propulsion concepts have been demonstrated in the past few years. For example, recent publications show that a spin stabilized Myrabo lightcraft reached 71 m in record height during vertical free flights outdoors,[M1] while a different parabolic flyer (design) was propelled from the ground of the laboratory to its 8 m high ceiling.[B2] High energy CO_2 lasers were used in both tests.

Researches using computational plasma aerodynamics have also been making progress in the field of laser propulsion. For example, Molvik et al.[M2] considered the interaction between a continuous laser beam and a flowing hydrogen gas using a structured-grid formulation and constant absorptivity. Jeng and Keefer[J1] did similar analysis with an expression for the absorption coefficient at CO_2 laser wavelength of 10.6 μm considering both electron-ion and electron-neutral inverse Bremsstrahlung. Conrad, et al.[C1] modeled a continuous optical discharge stabilized by nitrogen gas flows in weakly focused laser beam, using a absorption coefficient formula at 10.6 μm ignoring second ionization of atoms.[C1] Recently, Wang et al. performed transient performance calculations[W1] on a Myrabo lightcraft (energized by a pulsed laser beam) using an unstructured-grid formulation and the same single ionization absorption formula used by Conrad et al.[C1]

In a computational plasma aerodynamics study, using the modeling of a Myrabo lightcraft as an example, the focusing of the laser radiation is solved first, followed by computing the initial air breakdown and the creation of seed free electrons. When enough seed electrons are produced, they absorb more photons and resulting in more air breakdown and producing more free electrons. An avalanche of free electrons soon follows and a strong shock wave is generated. These are all solved with transport equations of continuity, energy, momentum, and species continuity, along with physical models such as finite-rate chemistry, high temperature thermodynamics, beam attenuation through absorption, beam refraction, and non-equilibrium radiation. The computational model then computes the subsequent traveling of the shock wave through air, the heating and ionizing of which (such that the air plasma becomes capable of absorbing more laser radiation), and most importantly of all, the thrust of the lightcraft propelled by the shock wave. Figure 1 shows a snapshot of the computed (heavy gas) temperature contours and laser beam traces at an elapsed time of 18 μs.[W1] It can be seen that the laser beam reflects specularly on the optical surface and focuses onto a focal "point" on the shroud where the breakdown of air starts. The temperature contours in Fig. 1 also describes the growth of the plasma front. The "protrusion" of the plasma front indicates that the plasma front (and the shock wave) is propagating up the beam – a result of successive heating and ionizing of the medium (air) such that the medium becomes capable of absorbing more laser energy and propagates further. Figure 1 is an indication of the potential ability of the computational plasma aerodynamics in describing the optical breakdown phenomenon associated with laser propulsion. It also indicates the importance of a realistic absorption model since the propulsion physics start with the absorption of laser energy. It goes without saying the accuracy of the absorption model affects that of the computed performance.

Other than the constant absorption coefficient used by Molvik et al.,[M2] all the variable absorption formulas used by the afore-mentioned modeling efforts[J1, C1, W1] are of the single ionization category. While applying single ionization formula to a hydrogen plasma[J1] is reasonable, there is room for improvement when it is applied to nitrogen and air plasmas,[C1, W1] since the atomic numbers of nitrogen and oxygen atoms are eight and nine, respectively. Given that the single ionization formula was formulated by Raizer and Tybulewicz[R1] in the 70's, while a simplified procedure for calculating an averaged degree of multiple ionization was reported by Zel'dovich and Raizer[Z1] in the 60's, and the same single ionization formula was still used in the 90's,[C1] led the author to speculate that the difficulty resides in the scarcity of reliable high temperature thermodynamic properties for the multiply ionized air atoms. To understand the impact of multiply ionized atoms on the absorption of laser radiation, reliable high temperature thermodynamic properties for the multiply ionized air atoms have to be developed, and that is the motivation of this study.

Thermophysics Characterization of Multiply Ionized air plasma

Thermo-Chemical System

In Ref. W1, the initial free electrons for plasma ignition and the subsequent avalanche of free electrons necessary for the optical breakdown were generated through the non-equilibrium, finite-rate air breakdown chemistry sub-model, where Park's multitemperature air chemistry mechanism[P3] was used. This mechanism

composes of the dissociation, NO exchange, associative ionization, charge exchange, electron impact ionization, and radiative recombination reactions. The eleven air plasma species used in this mechanism defines the thermo-chemical system for single ionization environment: N_2, O_2, NO, NO^+, N, N^+, O, O^+, N_2^+, O_2^+ and e^-. N_2, O_2, and NO are neutral molecules; N and O are neutral atoms; while NO^+, N^+, O^+, N_2^+, O_2^+ are single ions. In order to consider multiply ionized air plasma atoms, up to quadruple ionization, six additional ions N^{+2}, O^{+2}, N^{+3}, O^{+3}, N^{+4}, and O^{+4} must be added and their thermodynamic properties must be characterized.

Hydrogenic Approximation of the Partition Function

The high temperature thermodynamic properties of the six additional ions N^{+2}, O^{+2}, N^{+3}, O^{+3}, N^{+4}, and O^{+4} can be expressed in terms of partition functions, following those formulated for monatomic gases.[G2] For example,

$$\frac{C_p}{R} = T^2 \frac{d^2 \ln Q}{dT^2} + 2T \frac{d(\ln Q)}{dT} + \frac{5}{2}$$

$$\frac{H - H_0}{RT} = T \frac{d(\ln Q)}{dT} + \frac{5}{2}$$

$$\frac{S}{R} = T \frac{d(\ln Q)}{dT} + \ln Q + \frac{3}{2} \ln M + \frac{5}{2} \ln T + s_c$$

In this study, the partition functions of the multiply ionized atoms are characterized with the method of hydrogenic approximation.[Z1,J2] That is, the multiply ionized atoms are treated as hydrogen-like atoms, represented by a system consisting of a positive nucleus with a charge Z and a single electron. The transformed electronic partition takes the expression

$$Q_i = \Sigma_n 2n^2 \exp\left[-\frac{E_i}{kT} \left(1 - \frac{1}{n^2} \right) \right]$$

where the summation is truncated when $[E_i(1 - 1/n^2)]$ is greater than $[E_i - ZE_i]$. The lowering of the ionization potential is proportional to the square root of the sum of the electron density plus the ion densities times their charge squared divided by temperature. For consistency purpose, the high temperature thermodynamic properties of N, N^+, O, O^+ are also characterized as the hydrogen-like atoms.

The computational procedure is set up such that the internal energy and density are used as input. The internal energy of a given species is a function of the temperature, partition function, energy of ionization, and reference point energy. This reference is arbitrary, but it is chosen to be the energy of formation of the element from its reference state as defined in Gordon and McBride.[G2] The result of the computation is a table of thermodynamic properties for different atoms and multiply ionized ions as a function of temperature and pressures. Pressure is calculated from the ideal gas equation of state plus the Coulomb pressure correction.

Thermodynamic Function Generation

The next step is to construct the three thermodynamic functions of heat capacity, enthalpy and entropy as functions of temperature in a form compatible to most computational plasma aerodynamics codes. The standard form of Gordon and McBride[G2] is used:

$$\frac{C_p}{T} = a_1 T^{-2} + a_2 T^{-1} + a_3 + a_4 T + a_5 T^2 + a_6 T^3 + a_7 T^4$$

$$\frac{H}{RT} = -a_1 T^{-2} + a_2 T^{-1} \ln T + a_3 + a_4 \frac{T}{2} + a_5 \frac{T^2}{3} + a_6 \frac{T^3}{4} + a_7 \frac{T^4}{5} + \frac{b_1}{T}$$

$$\frac{S}{R} = -a_1 \frac{T^{-2}}{2} - a_2 T^{-1} + a_3 \ln T + a_4 T + a_5 \frac{T^2}{2} + a_6 \frac{T^3}{3} + a_7 \frac{T^4}{4} + b_2$$

These coefficients are obtained through a least-square curve-fit procedure for each temperature interval. Following Gordon and McBride[G2], three temperature intervals are used in this study. Unlike Gordon and McBride[G2], the three temperature intervals are made different for different species in order to achieve best fit of the generated thermodynamic properties, since the heat capacities of the multiply ionized atoms peak at vastly different temperatures. To construct the enthalpy curve, the heat of formation of multiply ionized ions at reference state needs to be estimated. This is accomplished by writing an ionization reaction, e.g., for N^+:

$$N \rightarrow N^+ + e^-$$

The heat of reaction of this ionization reaction is the ionization potential. The heat of formation of N^+ takes the form

$$H_{f,N^+} = H_{f,N} + E - H_{f,e^-}$$

For validation purpose, the calculated heat of formations for singly ionized N^+ and O^+ are comparable to those published in Gurvich et al.[G3] In addition, the calculated entropy of formations using hydrogenic

approximation of the partition function for N, O, N^+ and O^+ are also comparable to those published in Gurvich, et al. as well.

Figure 2 shows the computed heat capacities and curve fits for N, N^+, N^{+2}, N^{+3}, and N^{+4}, while Fig. 3 shows those for O, O^+, O^{+2}, O^{+3}, and O^{+4}. The peak heat capacity increases with temperature as the number of electrons stripped increases. The sensible heat capacities of the multiply ionized air plasma species cover a temperature range from 10,000 deg K to approximately 200,000 deg. K. The seven coefficients polynomials fit the computed heat capacities reasonably well.

The thermodynamic functions of the rest of the air plasma species (N_2, O_2, NO, NO^+, N_2^+, O_2^+ and e^-) can be found from Gordon and McBride[G4] where the calculated data from Gurvich et al.[G3] were curve-fitted. However, the applicable temperature range for these species were only calculated up to 20,000 deg K, as shown in Fig's 4-6. This temperature range appears to be too low, in light of the computed heavy gas and electron temperatures can go as high as 500,000 deg K during optical breakdown of air inside the focused region of a laser lightcraft.[W1] In addition, heat capacity data of many species do not level off to a value at higher temperatures, indicating possible overprediction of the heat capacity when extrapolated beyond 20,000 deg K. Nevertheless, there is no problem with electron since its heat capacity is a constant at any temperature. For species NO^+, N_2^+, and O_2^+, the low applicable temperature range does not present a problem either, since only trace amount of these species are produced at conditions of interest. For molecular species N_2, O_2, and NO, Balakrishnan reported correlations for specific heats up to 50,000 deg K.[B2] However, the formulas used by Balakrishnan were criticized as inadequate.[J3] Jaffe's calculated heat capacities for N_2, O_2, and NO were based on summations over all vibration-rotation energy levels for all known bound electronic states, and a scheme for the partitioning of the internal energy into vibrational, rotational and electronic contributions was presented which consistently accounts for the nonseparable nature of the various energy modes. Jaffe's work appears creditable and is used in this study.

Figures 4-6 show the heat capacities from all three sources for N_2, O_2, and NO, respectively. It can be seen that the heat capacities of Jaffe agree with those of Gordon and McBride reasonably well, while the heat capacities of Balakrishnan agree with those of the other two sources only at lower temperatures. The heat capacities of Jaffe are chosen for curve fitting for species N_2 and O_2. For species NO, Gordon and McBride's data were used for curve fitting up to 20,000 deg K, then Jaffe's heat capacities were fitted for the higher temperatures. Note that all three curves approach their asymptote values near 50,000 deg K, meaning these curves can be extrapolated to much higher temperatures, say, 500,000 deg K. It is a moot point though since these species do not survive beyond 20,000 deg K.

Laser Absorption

In computational plasma aerodynamics modeling[W1] of the laser lightcraft flowfield where geometric optics is used to simulate the local intensity of the laser beam, the laser beam can be split into a number of individual rays. In the presence of absorption, the local intensity of each ray follows the Beer's law:

$$\frac{dI_i}{ds_i} = -\kappa I_i$$

Through inverse Bremsstrahlung absorption, or free-free absorption, the rays are attenuated by free-electrons in its path. The three types of inverse Bremsstrahlung absorption, depending upon what kind of particle the electron is near when a photon is absorbed, are electron-ion, electron-atom, and electron molecular absorptions. According to Raizer and Tybulewicz,[R1] the long-wavelength infrared radiation of a CO_2 laser at 10.6 μm is absorbed mainly by free electrons when it collide with ions. Hughes[H1] gives a theoretical derivation of the electron-ion inverse Bremsstrahlung absorption coefficient for radiation at frequency ω:

$$\kappa_\omega = \frac{n_e n_i Z^2 e^6 g\left[1-\exp\left(-\hbar\omega/\kappa_B T\right)\right]}{\mu 6\varepsilon_0^3 c\hbar\omega^3 m_e^2}\left(\frac{m_e}{6\pi\kappa_B T}\right)^{1/2}$$

The advantage of Hughes' formula is its flexibility. That is, it can be used for radiation in any wavelength. In contrast, started with a different formulation from that of Hughes, corrected for stimulated emission in the single ionization range, assumed $\hbar\omega/\kappa_B T << 1$, omitted the factor affecting only the photoionization, substituted $\hbar\omega$ for CO_2 laser wavelength, a formula of electron-ion inverse Bremsstrahlung absorption coefficient is expressed by Raizer and Tybulewicz:[R1]

$$\kappa_{CO_2} = \frac{10.4 p_e^{\,2} g}{(T/10^4)^{7/2}}$$

where

$$g = 0.55\ln\left[27\left(T/10^4\right)^{4/3} p_e^{-1/3}\right]$$

Note the above absorption coefficient formula does not

take the second ionization (or higher) into account. Also, electron pressure is used in lieu of electron number density. Both formulas described above consider only the electron-ion inverse Bremsstrahlung absorption. On the other hand, Mertogul[M3] computed the absorption coefficient using all three types of inverse Bremsstrahlung. The formula used for the calculation of electron-ion inverse Bremsstrahlung absorption coefficient is that given by Stallcop:[S1]

$$\kappa_\omega = n_e n_i \left(\frac{256}{3}\right)\left(\frac{\pi}{3}\right)^{1/2} \pi^2 \alpha a_0^5 \left(\frac{E}{h\omega}\right)^3 \left(\frac{E}{\kappa_B T}\right) \left[1 - \exp\left(-\frac{h\omega}{\kappa_B T}\right)\right] g$$

in which the free-free Gaunt factor was curve fitted form reported data of Karzas and Latter at wavelength of 10.6 μm and T < 10,000 deg K:

$$g = 1.07 + 6.9643x10^{-5}T - 2.6786x10^{-9}T^2$$

and for T > 10,000 deg K:

$$g = 1.50 + 1.0x10^{-5}T$$

The expression used for the electron-atom inverse Bremsstrahlung absorption coefficient in the infrared limit is that given by Stallcop:[S2]

$$\kappa_\omega = n_e n_a \kappa_B T \left(2.15x10^{-29}\right)\left(\frac{E}{h\omega}\right)^2 \frac{\exp(-4.862k_T(1 - 0.2096k_T + 0.017k_T^2 - 0.00968k_T^3)}{k_T}$$

and

$$\kappa_T = \left(\frac{\kappa_B T}{E}\right)^{1/2}$$

The expression used for the electron-molecule inverse Bremsstrahlung absorption coefficient is that given by Caledonia et al.[C2] from the work of Dalgarno and Lane:[D1]

$$\kappa_\omega = n_e n_m \left(4.51x10^{-44}\right) \frac{D}{T^{3/2}\left[1 - \exp\left(-\frac{h\omega}{\kappa_B T}\right)\right]}$$

where D is a complicated power series represented as a function of $h\omega/\kappa_B T$ and was given in a Appendix of Mertogul.[M3] For a CO_2 laser wavelength of 10.6 μm, this expression of electron-molecule inverse Bremsstrahlung absorption coefficient is only valid for temperatures less than 4321.5 deg K. In addition, Mertogul's formula was derived for hydrogen plasma, a deviation from our interest in air breathing laser propulsion. Nevertheless, Mertogul's formula is included in this study to compare the relative importance of these three types of inverse Bremsstrahlung absorption.

Results and Discussion

Thermodynamic functions generated in this study for multiply ionized ions, atoms, and molecules are used as data base for a series of constant pressure (1 atmosphere) and temperature thermal equilibrium computations, in order to obtain the necessary compositions of electron, ions, atoms and molecules for laser absorption coefficient calculations. In the temperatures of interest, equilibrium state is probably a reasonable assumption. Minimization of free energy of a thermo-chemical system, similar to that described in Gordon and McBride,[G4] is used as the algorithm for achieving the equilibrium state and is not repeated in here. Figure 7 shows the air plasma species compositions considering single ionization only. As temperature increases, the molecules disappear quickly and atoms emerge. And then atoms disappear, while electron and ions (N^+ and O^+) rise, eventually, the species concentrations of electron and ions level off at about 32,000 deg K. The final electron mole fraction of 0.5 is the result of single ionization. Note that the concentrations of NO^+, N_2^+, and O_2^+ are indeed negligible.

Figure 8 shows the comparison of calculated absorption coefficients of air for CO_2 laser radiation using the information from Fig. 7. Also plotted in Fig. 8 are points read off from Fig. 6.18 of Raizer and Tybulewicz[R1] while allowing for double ionization. At low temperatures, the calculated absorption coefficients are extremely low and rise sharply with increasing temperate around 8000 deg K. The rise then slows down and the absorption passes through a maximum. The calculated absorption drops monotonically from the maximum as the system completes the single ionization, eventually nearing zero absorption around 80,000 deg K.

It can be seen that the curves using Raizer and Tybulewicz formula and that of Hughes are reasonably close, although the peak value of Hughes is higher. The peak value of Mertogul is the lowest among the three. This is not surprising since Mertogul's formula was meant for hydrogen plasma. Of interest is at lower temperatures where the electron-atom, and electron-

molecular inverse Bremsstrahlung absorptions should show some contribution, but none was observed, indicating the free-free inverse Bremsstrahlung absorption is indeed the main absorption process among the three as described by Raizer and Tybulewicz.

On the other hand, the curve of Hughes Formula agrees better with data points from Fig. 6.18 of Raizer and Tybulewicz than that calculated using Raizer and Tybulewicz formula, until the second ionization takes place. This is somewhat perplexing and it is speculated that difference in generating the electron pressures may have been the problem. Raizer and Tybulewicz did not elaborate how the electron pressure was obtained, nor did they explain how the second ionization portion was arrived and only the single ionization formula was given. Nevertheless, the mathematical reason for the monotonic decrease of the calculated absorption coefficient after the passing of the maximum can be seen clearly from Fig. 7 that electron partial pressure is a constant as temperature exceeds 30,000 deg K, that the Gaunt factor is essentially a constant since it ranges from 2.3 to 3.2 in the temperature range of interest, and that the denominator of Raizer and Tybulewicz formula eventually grows as temperature increases. The downward trend of all three curves after their peaks confirms the single ionization system does not produce a second rise in absorption coefficient.

Although only reported to 27,000 deg K,[R1] the importance of second ionization is evident from Fig. 8 in which the single ionization formulas under-predict the absorption coefficient at high temperatures where double ionization occurs. This has strong implications for laser lightcraft performance computations using computational plasma aerodynamics. The implication of double ionization also implies the potential importance of triple ionization, ..., etc. That raises an issue of rising computational cost if too high a degree of ionization is considered however, for the computational cost is proportional to the square of the number of species considered.

Based on the result in Fig. 8, the general Hughes formula is used to investigate the effect of multiple ionization, in conjunction with the Gaunt factor given by Raizer and Tybulewicz. This is accomplished by performing a series of equilibrium computations using the characterized thermodynamic properties for multiply ionized air ions N^{+2}, O^{+2}, N^{+3}, O^{+3}, N^{+4}, and O^{+4}. The plasma composition required for absorption calculation is obtained by increasing the degree of ionization sequentially, up to quadruple ionization.

Figures 9-11 show the equilibrium air plasma species compositions for double, triple, and quadruple ionizations, respectively. As expected, the surviving ions for double ionization are N^{+2} and O^{+2} for temperatures exceeding 50,000 deg K, those for triple ionization are N^{+3} and O^{+3} for temperatures exceeding around 95,000 deg K, and those for quadruple ionization are N^{+4} and O^{+4} for temperatures exceeding 100,000 deg K. The peaks of those multiply ionized species concentration decrease as the degree of ionization increases. Most importantly, the mole fractions of the free electron increase from 0.5 for single ionization, to 0.67, 0.75, and 0.8 for double, triple, and quadruple ionizations, respectively.

Figure 12 shows the comparison of electron number densities for double, triple, and quadruple ionizations. A second peak of the electron number density occurs at around 30,000 deg K, due to the double ionization. Triple ionization increases the overall electron number density from approximately 40,000 degree up. Quadruple ionization increases the electron number density from around 65,000 degree up, but the amount of increase becomes less as the degree of ionization increases. That indicates for computational purpose, quadruple ionization is probably enough.

Figure 13 shows the comparison of calculated absorption coefficient curves for double, triple, and quadruple ionizations. A second maximum in the absorption coefficient at temperatures near 30,000 deg K occurs due to double ionization. As the system completes the second ionization, the absorption again passes a maximum, although it is much less obvious as the last peak, and so on. The earlier part of the second ionization curve agrees well with the available points from Raizer and Tybulewicz. Note that the area under the quadruple ionization curve is about twice that of the single ionization. In summary, under a single ionization system, the absorption of photons drops sharply beyond 25,000 deg K and appears to cease absorbing energy at 80,000 deg K. When allowing for quadruple ionization, the absorption not only passes through multiple maximums, but also continues to absorb energy beyond 100,000 deg K.

Conclusions

A thermophysics characterization of inverse Bremsstrahlung absorption of laser radiation is performed. Thermo-chemical properties of multiple ionized air plasma species are generated using hydrogenic approximation of the electronic partition function and those for neutral air molecules are also generated using updated literature data. Three formulas for absorption are calculated and a general formula is recommended for multiple ionization absorption calculation. A series of thermal equilibrium computations are performed to show the effect of multiple ionization on the free electron concentration and on the inverse Bremsstrahlung absorption coefficient. The calculated second ionization absorption coefficient agrees

reasonably well with available data of literature. In addition, it is found that the area under the quadruple ionization curve of absorption is about twice that of the single ionization. The result of this study can be applied to the computational plasma aerodynamics modeling of laser propulsion physics.

Acknowledgments

The lead author wishes to thank John Cole of Revolutionary Propulsion Research for supporting this study. He also wishes to thank Drs. Yen-Sen Chen and Jiwen Liu for discussions on the laser absorption coefficients.

References

[K1] Kantrowitz, A., "Propulsion to Orbit by Ground-Based Lasers," *Astronautics and Aeronautics*, Vol. 10, No. 5, May 1972, pp. 74-76.

[P1] Pirri, A.N., Monsler, M.J., and Nebolsine, P.E., "Propulsion by Absorption of Laser Radiation," *AIAA Journal*, Vol. 12, No. 9, 1974, pp. 1254-1261.

[G1] Glumb, R.J., and Krier, H., "Concepts and Status of Laser-Supported Rocket Propulsion," *Journal of Spacecraft and Rockets*, Vol. 21, No. 1, 1984, pp. 70-79.

[B1] Brandstein, A., and Levy, Y., "Laser Propulsion System for Space Vehicles," *Journal of Propulsion and Power*, Vol. 14, No. 2, 1998, pp. 261-269.

[P2] Phipps, C.R., Reilly, J.P., and Campbell, J.W., "Optimum Parameters for Laser Launching Objects into Low Earth Orbit," *Laser and Particle Beams*, Vol. 18, 2000, pp. 661-695.

[M1] Myrabo, L.N., "World Record Flights of Beam_riding Rocket Lightcraft: Demonstration of "Disruptive" Propulsion Technology," AIAA Paper 2001-3798, July, 2001.

[B2] Bohn, W.L., "Laser Lightcraft Performance," *High Power Laser Ablation II*, Proceedings of SPIE, Vol. 3885, 2000, pp. 48-53.

[M2] Molvik, G.A., Choi, D., and Merkle, C.L., "A Two-Dimensional Analysis of Laser Heat Addition in a Constant Absorptivity Gas," *AIAA Journal*, Vol. 23, No. 7, 1985, pp. 1053-1060.

[J1] Jeng, San-Mou, and Keefer, Dennis, "Theoretical Evaluation of Laser-Sustained Plasma Thruster Performance," *Journal of Propulsion*, Vol. 5, No. 5, Sept-Oct., 1989, pp. 577-581.

[C1] Conrad, R., Raizer, Y.P., and Surzhikov, S.T., "Continuous Optical Discharges Stabilized by Gas Flow in Weakly Focused Laser Beam," *AIAA Journal*, Vol. 34, No. 8, 1996, pp. 1584-1588.

[W1] Wang, T.-S., Chen, Y.-S., Liu, J., Myrabo, L.N., and Mead, F.B. Jr., "Advanced Performance Modeling of Experimental Laser Lightcraft," AIAA Paper 2001-0648, 39th AIAA Aerospace Sciences Meeting & Exhibit, Jan. 8-11, Reno, NV, 2001.

[R1] Raizer, Y.P., and Tybulewicz, A., "Laser-Induced Discharge Phenomena", *Studies in Soviet Science*, Edited by Vlases, G.C., and Pietrzyk, Z.A., Consultants Bureau, New York, 1977.

[Z1] Zel'dovich, Y.B., and Raizer, Y.P., "Physics of Shock Waves and High Temperature Hydrodynamic Phenomena", Vol. 1, Edited by Hayes, W.D., and Probstein, R.F., Academic Press, New York and London, 1966.

[P3] Park, C., "Review of Chemical-Kinetic Problems of Future NASA Missions, I: Earth Entries," *Journal of Thermophysics and Heat Transfer*, Vol. 7, No. 3, 1993, pp. 385–398.

[G2] Gordon, S., and McBride, B.J., "Thermodynamic Data to 20,000 K for Monatomic Gases," NASA TP 1999-208523, Glen Research Center, Cleveland, Ohio, June 1999.

[J2] Richter, J., "Radiation of Hot Gases," *Plasma Diagnostics*, edited by Lochte-Holtgreven, W., John Wiley & Sons, New York, 1968, pp. 1-32.

[G3] Gurvich, L.V., Veyts, I.V., and Alcock, C.B., "Thermodynamic Properties of Individual Substances," Fourth Edition, Part Two, Hemisphere Publishing Co., New York, 1989.

[G4] Gordon, S., and McBride, B.J., "Computer Program for Calculation of Complex Chemical Equilibrium Compositions and Applications," NASA RP 1311, Lewis Research Center, Cleveland, OH, 1996.

[B2] Balakrishnan, A., "Correlations for Specific Heats of Air Species to 50,000 K," AIAA Paper 86-1277, June 1986.

[J3] Jaffe, Richard, "The Calculation of High-Temperature Equilibrium and Nonequilibrium Specific Heat Data for N_2, O_2, and NO," AIAA Paper 87-1633, June 1987.

[H1] Hughes, T.P., "Plasma and Laser Light", John Wiley and Sons, New York, 1975.

[M3] Mertogul, A.E., "Modeling and Experimental Measurements of Laser Sustained Hydrogen Plasmas," Ph.D. Thesis, University of Illinois at Urbana-Champaign, 1993

[S1] Stallcop, J.R., "Absorption of Laser Radiation in a H-He Plasma. I. Theoretical Calculation of the Absorption Coefficient," *Physics of Fluids*, Vol. 17, No. 4, pp. 751-758, April 1974.

[K2] Karzas, W.J., and Latter, R., "Electron Radiative Transitions in a Coulomb Field," *Astrophysical Journal, Supplement Series, Supplement number 55*, Vol. VI, pp. 167-211, 1961.

[S2] Stallcop, J.R., "Absorption of Infrared Radiation by Electrons in the Field of a Neutral Hydrogen Atom," *Astrophysical Journal*, Vol. 187, No. 1, pp. 178-183, Jan. 1974.

[C2] Caledonia, G.E., Wu. P.K.S., and Pirri, A.N.,

"Radiation Energy Absorption Studies for Laser Propulsion," NASA CR-134809, March 1975.

[D1] Dalgarno, A., and Lane, N.F., "Free-Free Transitions of Electrons in Gases," *Astrophysical Journal*, Vol. 145, No. 2, pp. 623-633, July 1966.

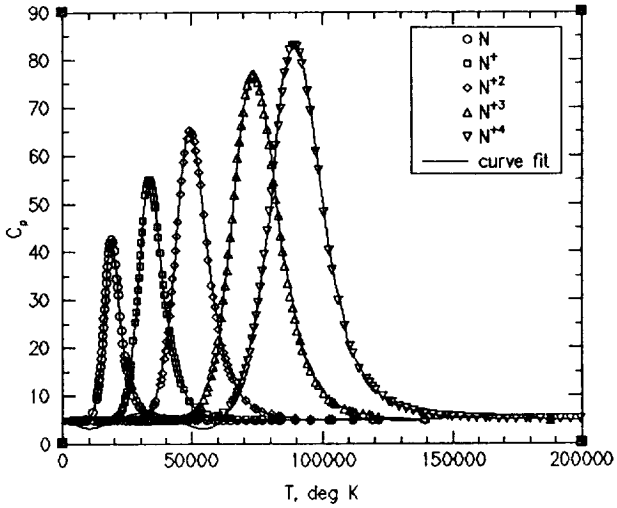

Fig. 2 Computed heat capacities and curve fits for multiply ionized nitrogen atoms N, N^{+}, N^{+2}, N^{+3}, and N^{+4}.

Fig. 1 Computational plasma aerodynamics computed temperature contours and laser ray traces for a Myrabo lightcraft at 18 μs. Contours scale: 0 – 24180.

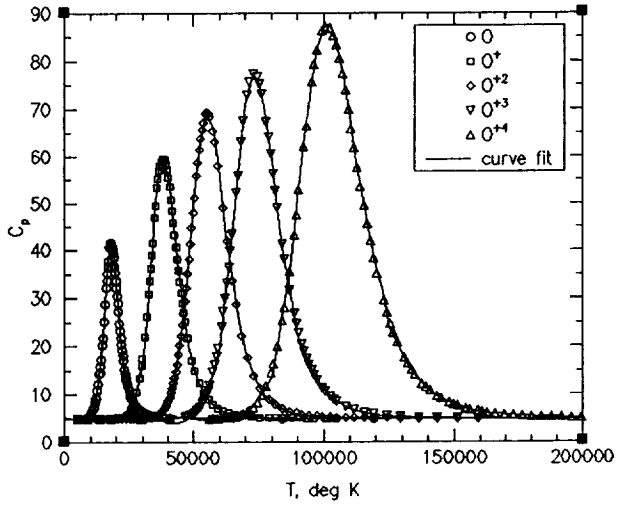

Fig. 3 Computed heat capacities and curve fits for multiply ionized oxygen atoms O, O^{+}, O^{+2}, O^{+3}, and O^{+4}.

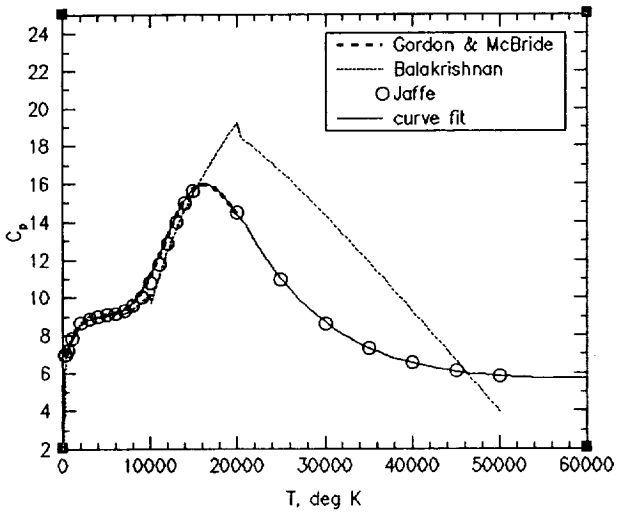

Fig. 4 A comparison of the heat capacities and curve fit for neutral N_2.

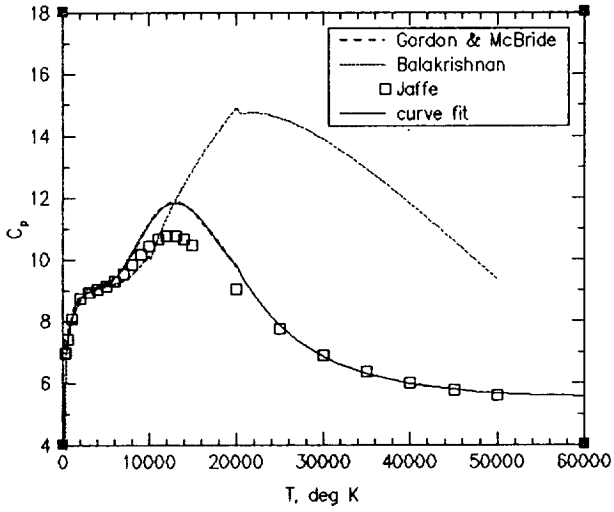

Fig. 6 A comparison of the heat capacities and curve fit for neutral molecule NO.

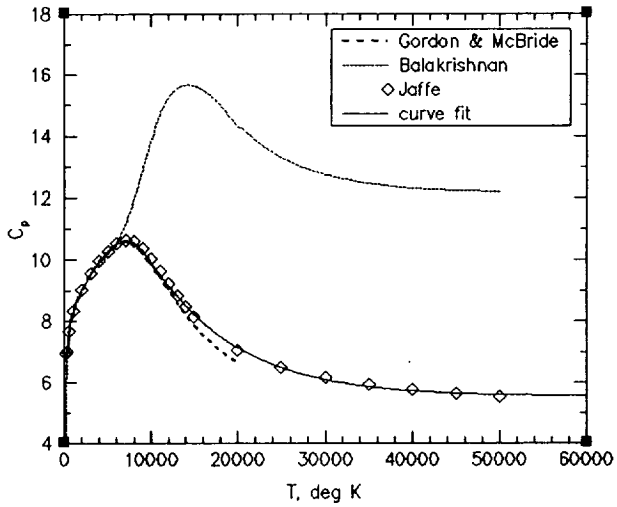

Fig. 5 A comparison of the heat capacities and curve fit for neutral molecule O_2.

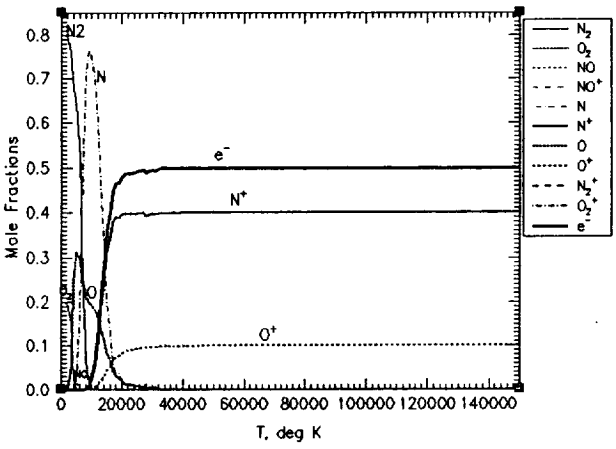

Fig. 7 A comparison of the equilibrium air plasma species compositions for single ionization.

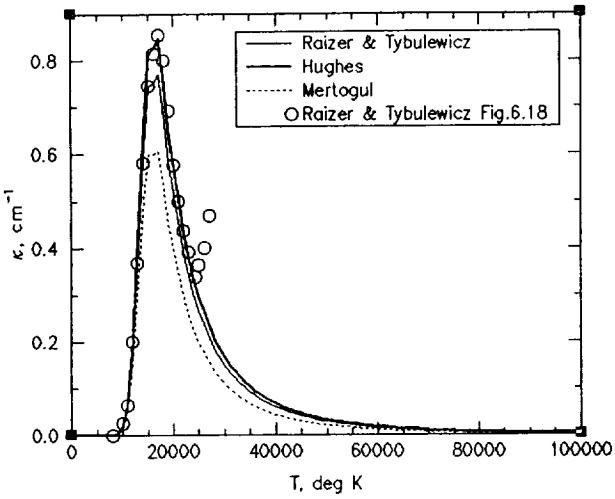

Fig. 8 A comparison of the calculated absorption coefficients of air.

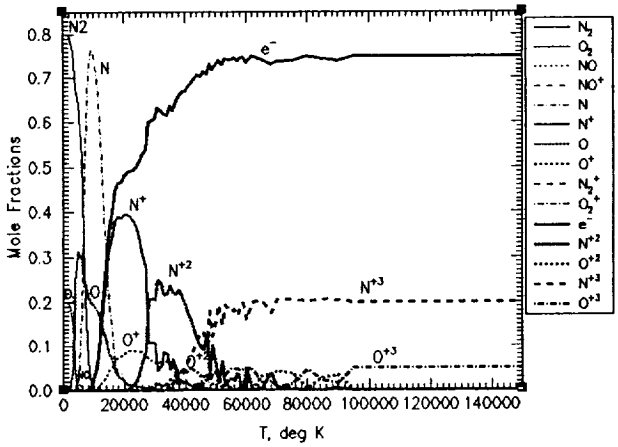

Fig. 10 A comparison of the equilibrium air plasma species compositions allowing for triple ionization.

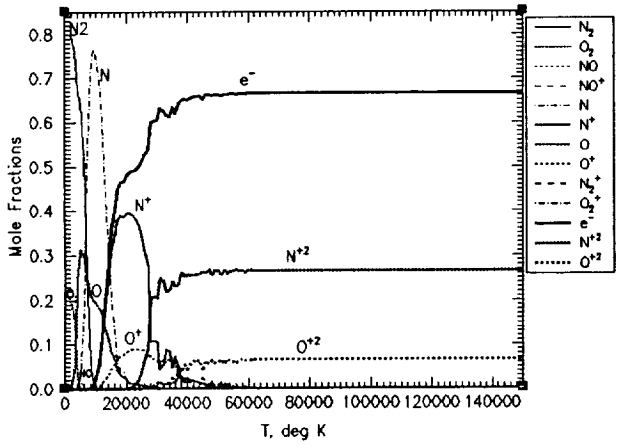

Fig. 9 A comparison of the equilibrium air plasma species compositions allowing for double ionization.

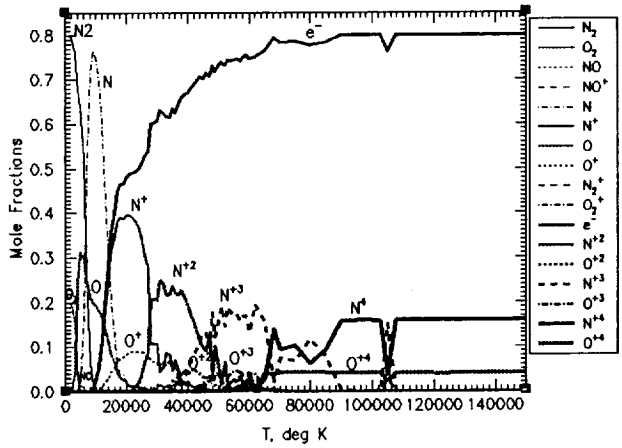

Fig. 11 A comparison of the equilibrium air plasma species compositions allowing for quadruple ionizations.

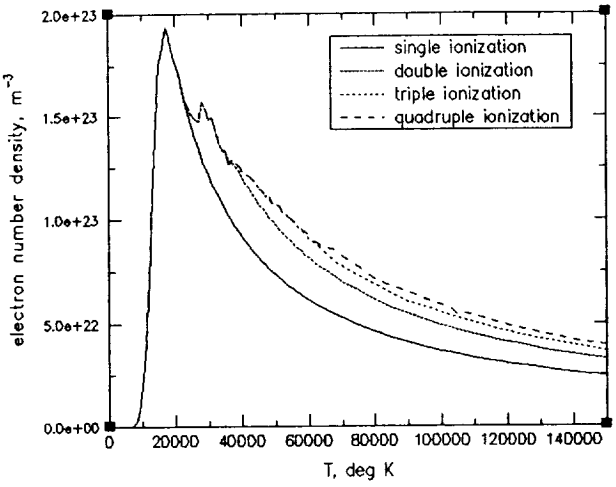

Fig. 12 A comparison of the electron number densities for double, triple, and quadruple ionizations.

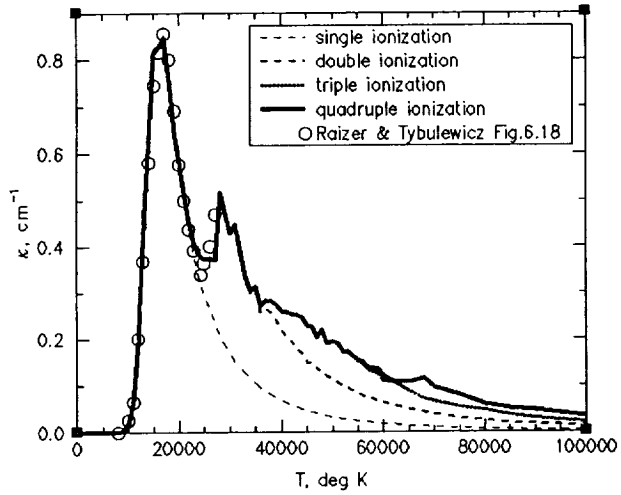

Fig. 13 A comparison of calculated absorption coefficients for double, triple, and quadruple ionizations.